

Rapid Cascade Synthesis of Poly-Heterocyclic Architectures from Indigo

Alireza Shakoori,[†] John B. Bremner,[†] Anthony C. Willis,[‡] Rachada Haritakun,[§] and Paul A. Keller^{*,†}

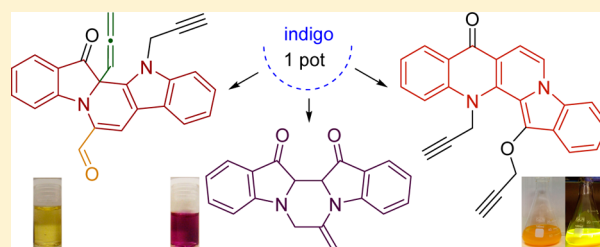
[†]School of Chemistry, University of Wollongong, Wollongong, NSW, 2522, Australia

[‡]School of Chemistry, The Australian National University, Canberra, ACT 0200, Australia

[§]National Centre for Genetic Engineering and Biotechnology (BIOTEC), National Science and Technology Development Agency (NSTDA), 113 Phaholyothin Road, Klong1, Klong Luang, Pathumthani 12120 Thailand

Supporting Information

ABSTRACT: The base-induced propargylation of the dye indigo results in the rapid and unprecedented one-pot synthesis of highly functionalized representatives of the pyrazino[1,2-*a*:4,3-*a'*]-diindole, pyrido[1,2-*a*:3,4-*b'*]diindole and benzo[*b*]indolo[1,2-*h*]-naphthyridine heterocyclic systems, with the last two reflecting the core skeleton of the anticancer/antiplasmodial marine natural products fascaplysin and homofascaplysin and a ring B-homologue, respectively. The polycyclic compounds 6–8, whose structures were confirmed through single-crystal X-ray crystallographic analysis, arise from sequential inter/intramolecular substitution–addition reactions, and in some cases, ring rearrangement reactions. Preliminary studies on controlling the reaction path selectivity, and the potential reaction mechanisms, are also described. Initial biological activity studies with these new heterocyclic derivatives indicated promising in vitro antiplasmodial activity as well as good anticancer activity. The chemistry described is new for the indigo moiety and cascade reactions from this readily available and cheap starting material should be more broadly applicable in the synthesis of additional new heterocyclic systems difficult to access by other means.



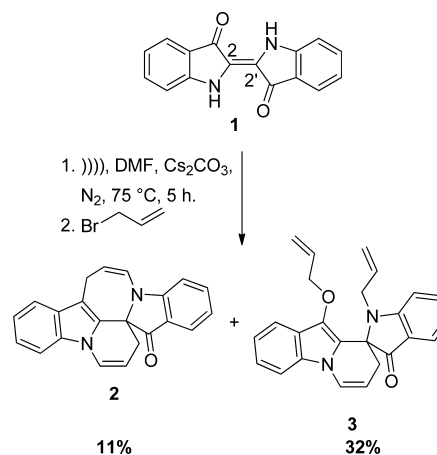
INTRODUCTION

One of the current goals in organic synthesis is the controlled construction of complex molecules, in particular, through the use of cascade reaction sequences.¹ Such molecular explorations, yielding novel architectures, are of particular interest for the investigation of new bioactive agents with possible new modes of action, which could be subsequently elaborated in medicinal chemistry programs.² Approaches to the realization of these synthetic goals have often been explored in the context of complex multistep syntheses of natural product targets.³ Our focus has been on the smaller, though versatile, canvas, of the abundant and cheap natural product, indigo 1 (Scheme 1).

There is significant advantage in starting with a readily available advanced precursor such as indigo: its reported chemistry is very limited despite the presence of an array of closely positioned functionality in the 2,2'-diindolic unit which allows for cascade reaction paths. It also provides a unique opportunity in providing an advanced starting material for the potential rapid synthesis of the diindolic system of natural products analogs. Such biologically active natural products (e.g., with anticancer or antimicrobial activity) include fascaplysin,⁴ homofascaplysin,⁵ iheyamines,⁶ staurosporine,⁷ and rebeccamycin⁸ (Figure 1).

To explore our synthetic approach, we initially investigated the base-mediated reactions of indigo with allylic halides, which in the case of allylic bromide resulted in the rapid synthesis of the multicyclic compounds 2 and 3 (Scheme 1).⁹ These

Scheme 1. Allylation of Indigo



compounds represent new ring systems with functionality suitable for further elaboration of molecular complexity.

In an extension of this work and in an investigation of reaction directing elements, particularly those modulating nucleophilic–electrophilic reactivities, we have studied the base-induced reactions of indigo with the simple alkyne analog,

Received: June 5, 2013

Published: June 26, 2013

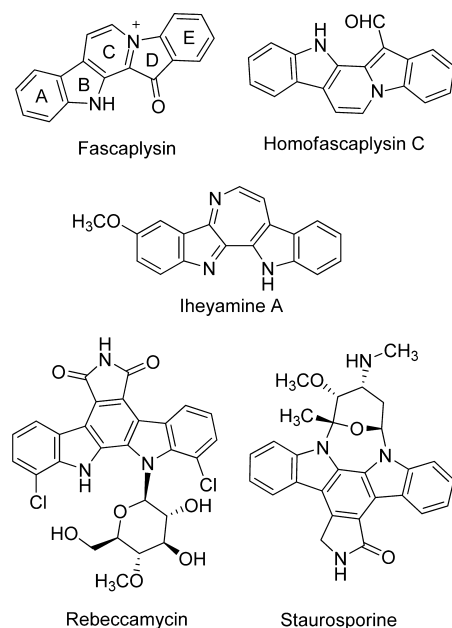


Figure 1. Some biologically active natural products with an embedded 2,2'-diindolic unit.

propargyl bromide. New facile routes to the core heterocyclic system of fascaplysin, homofascaplysin, and the B-ring homologue of this system were discovered and the results are reported in this paper together with some initial *in vitro* antiparasitoid and anticancer activity data.

RESULTS AND DISCUSSION

Synthesis and Structural Elucidation. Our previous experience in the chemistry of indigo⁹ revealed that relatively small changes to reaction conditions could have major impacts on the product outcome. Therefore, our attempts at the propargylation of indigo paid particular attention to stringent and repeatable reactions conditions. In this context, a solution of indigo in DMF was generated through sonication for 30 min at room temperature and then transferred to a septum-equipped flask which contained predried molecular sieves and cesium carbonate under an inert atmosphere. The flask was then plunged into a preheated oil-bath (strictly 85–87 °C) and stirred for 30 min, followed by the addition of propargyl bromide and the reaction mixture heated at this temperature for 5 min. Following quenching, a sequence of separations yielded the five new products 4–8 in a combined yield of 81% (Scheme 2).

The expected mono *N*-substituted indigo derivative (4) was isolated as a deep blue, papery solid in 11% yield after silica-gel column chromatography. Data from the HRESI mass spectrum was consistent with the molecular formula of 4 and was indicative of the addition of one propargyl unit. ¹H NMR NOE analysis also confirmed the presence of the expected *trans* isomer. In a separate reaction, under analogous conditions but with a very short reaction time (<1 min) and a stoichiometric quantity of propargyl bromide, compound 4 could be isolated in a much improved 93% yield (Scheme 3, Step A). The increased solubility in a range of organic solvents (e.g., THF, CH₂Cl₂) enables this monopropargylated material to be used as a starting material for subsequent reactions, including cyclizations. This increased flexibility in the use of solvents allows for a greater variation in reaction conditions to be used.

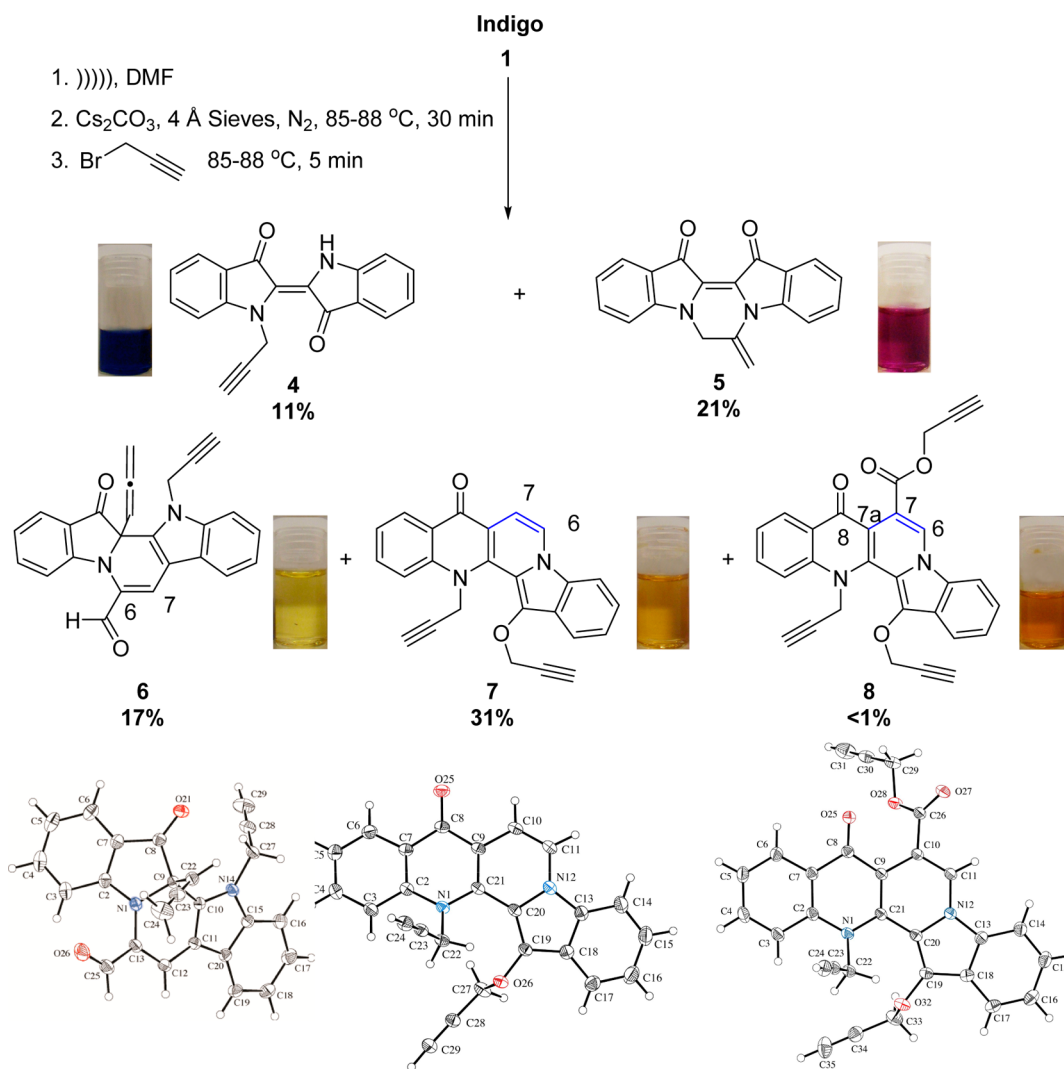
The pyrazinodiindole 5 (Scheme 2) was isolated in 21% yield as a red–burgundy solid. The ¹H NMR spectrum showed singlets at 5.04 and 5.38 ppm, assigned to the exocyclic methylene protons whereas the ¹³C NMR spectrum showed 2 peaks at 179.7 and 180.8 ppm, assigned to two nonequivalent carbonyls. Data from the HRESI mass spectrum was supportive of the molecular formula of 5 and was indicative of the addition of one propargyl unit.

The UV–vis spectrum of 5 had a strong adsorption band with a maximum at 324 nm ($\epsilon = 13\,088$). The burgundy color was suggestive that the central double bond of indigo remained intact, with all other indigo derivatives in which this bond had been converted to a single bond appearing as yellow compounds. Simple modeling studies (Spartan, Wave function) indicated that compound 5, while planar through the indigo moiety, positioned the hydrogen atoms of the endocyclic methylene group above and below the plane of the molecule with the exocyclic methylene twisted out of the molecule plane.¹⁰ This product 5 can also be synthesized in high yield (98%) by the reaction of 4 in DMF in the presence of Cs₂CO₃ (Scheme 3, Step B).

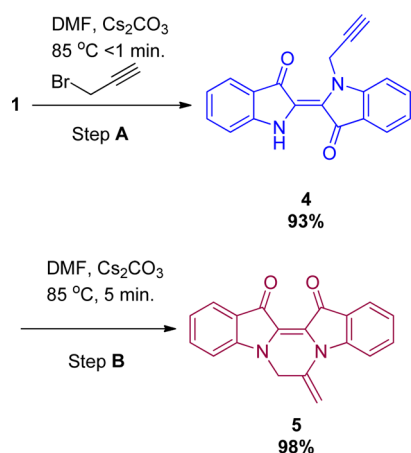
The pyridodiindole 6 (Scheme 2) was isolated in 17% yield as yellow–orange crystals. Analysis of the ¹H NMR indicated a peak at 9.62 ppm assigned to the aldehyde proton, and a doublet at 4.79 ppm ($J = 6.5$ Hz) assigned to the terminal protons of the allene moiety and a singlet at 2.33 assigned to the terminal alkyne proton. The ¹³C NMR spectrum showed peaks at 90.4, 208.4, and 80.4 ppm, assigned sequentially to the three allene carbons from the CH. A peak at 195.7 ppm was assigned to the aldehyde. The HRESI mass spectrum of 6 was consistent with a molecular formula of C₂₅H₁₆N₂O₂. The molecular structure was confirmed as 6 by X-ray crystallographic analysis, together with the disposition of the allene group over the pyrido ring rather than pointing away from it (Scheme 2). There is one stereogenic carbon present at C12a, but in the absence of any chiral element during the reaction, the stereochemical outcome was a racemic mixture, as confirmed by optical rotation analysis. The structure of 6 poses interesting mechanistic questions. The addition of three propargyl units is evidenced by the presence of the allene, the *N*-propargyl unit and the three-carbon moiety encompassing the aldehyde, and C6 and C7. Interestingly, this three-carbon unit is attached to the indigo N at the middle carbon, and not through the propargyl bromide methylene or the terminal alkyne positions.

The major product of the reaction was the benzoindolophthalidinone 7 (Scheme 2) isolated in 31% yield as a yellow solid which was also highly fluorescent in CH₂Cl₂ solution with a brilliant yellow color under UV light (365 nm). The ¹H NMR showed two pairs of doublets at 8.01 and 7.33 ppm ($J = 7.4$ Hz) assigned to H6 and H7, respectively. Two singlets at 2.14 and 2.30 ppm were assigned to the terminal acetylenic protons with the corresponding propargyl methylenes assigned to the doublets at 4.74 and 5.49 ppm ($J = 2.4$ Hz). A comparative analysis of the NMR and mass spectra indicated that although two substituent propargyl units were present, the molecular ion indicated the addition of three propargyl units, the last being incorporated into a ring (Scheme 2, 7, blue). The structure of 7 was confirmed by X-ray crystallographic analysis. The ring expansion of the indigo 5-membered ring into a 6-membered ring is new chemistry, with the three additional carbons of the indolo[1,2-*h*][1,7]naphthyridine parent structure being sourced from the additional propargyl unit. Retrosynthetically, sourcing the C6–C7–C7a moiety from a propargyl unit with the

Scheme 2. Base-Mediated Propargylation of Indigo to Produce the Heterocyclic Compounds 4–8 (Adjacent to Each Structure Is Illustrated a Solution, Highlighting the Color)



Scheme 3. Synthesis of **4** and Subsequent Conversion to **5**



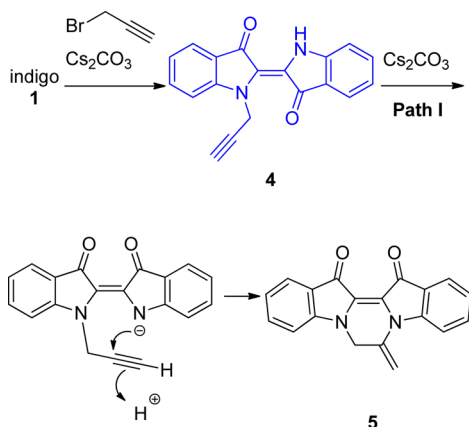
remaining skeleton from indigo is not intuitive and highlights the novelty of this new chemistry of indigo. The final product, isolated in very low yield (<1%), was the yellow benzoin-dol-naphthyridinone **8** (Scheme 2), with the structure confirmed by single-crystal X-ray analysis.

Color is an important qualitative element in the structural elucidation of these polycyclic compounds. The disappearance of the blue and emergence of yellow appears to indicate the loss of H-bonding between the indigo carbonyl and the NH, along with loss of unsaturation in the indigo central bond and the presence of either sp³ hybridized carbon atoms (e.g., **6**), or extended fused ring systems, e.g. heterocycles **7** or **8**. The mono-*N*-propargylated **4**, with both structural elements still present, maintains the deep blue intensity, whereas the cyclized structure **5**, which still contains the central double bond but has lost the H-bonding, is a burgundy color (Scheme 2).

Mechanistic and Reaction Discussion. The proposed mechanisms for the propargylation of indigo are summarized in Schemes 4–6 and involve five key pathways. The pyrazino-diindole **5** is derived from the monopropargylated indigo **4** (blue, Path I, Scheme 4, and Scheme 3) after *N*-deprotonation, followed by delocalization allowing rotation around the central bond to the cisoid conformation. Subsequent intramolecular nucleophilic addition to the propargyl C2 position yields **5** (Scheme 4).

Path II starts with the identical key intermediate **4** (blue, Scheme 5) undergoing prototropic tautomerism (A) which subsequently *N*-alkylates (B). Deprotonation of the *N*-

Scheme 4. Proposed Mechanism for Formation of 4 and 5 (Colored Structures Indicate Common Intermediates in the Overall Mechanism and Are the Same within Schemes 5 and 6)



methylene generates a stabilized ylid, which allows cyclization onto the carbonyl generating an activated cyclic allene intermediate (C). Under standard conditions, an “alkyne nucleophile” is insufficiently strong to attack an electrophilic carbonyl in the absence of a metal (e.g., Au, Ru) or an activating influence. In this instance, the anion from the ylid serves as a formal negative charge allowing this cyclization to the 7-ring allene to occur. A comprehensive review on allenes from 1989¹¹ reported the isolation of an eight-membered carbocyclic allene, however, the corresponding six-membered rings have been plausibly demonstrated as reactive intermediates.¹² Further, with the seven-membered carbocyclic allene, isodesmic reaction energy calculations indicate¹³ an allene strain component of 13.5–14.3 kcal/mol, consistent with its ready preparation and trapping. Heterocyclic allenes have also been isolated as small as eight-membered rings, with a mixed

“P” and “B” heteroatom ylid.¹⁴ Therefore the postulated cyclic allene intermediate C (Scheme 5) is reasonable.

The cyclic allene could then undergo a ring-expansion reaction, to produce the benzo[*b*]indolo[1,2-*h*][1,7]-naphthyridin-8-(13*H*)-one ring structure D (Scheme 5). The proposed driving force behind this ring-expansion is relief of ring strain of the 7-membered allenic ring—therefore, there is a favorable energy balance between the 7-membered allenic ring formation, and its subsequent role in providing a driving force for ring expansion. An additional crucial component of this step is the presence of an electrophile (E)—the major product arising from the reaction, 7, requires E = H⁺, whereas the minor product 8 requires E = CO₂, probably generated, on the basis of the results noted in Table 1, from carbonic acid decomposition, the acid in turn resulting ultimately from the Cs₂CO₃ base via bicarbonate (see below for a greater discussion). Once the carboxylate unit is incorporated, a further propargyl moiety could be added via nucleophilic displacement to produce the ester substituent of 8. Subsequent dehydrogenation, followed by base-induced aromatization allows for *O*-propargylation in a cascade process, yielding the final products 7 (Path III) and 8 (Path IV)(Scheme 5).

The addition of a 1-carbon unit is novel and imposes the question as to the origin of this carbon, even though 8 is isolated in very low yield. Two possibilities arise and involve either the well-known degradation of DMF¹⁵ to produce a “C=O” fragment that could be incorporated, or it could arise from the generated bicarbonate anion that is present in the solution. Table 1 summarizes experiments to determine the source of the additional carbon atom in 8. Entry 1 is the standard reaction as previously outlined, whereas entry 2 describes replacing the DMF solvent with DMSO—this resulted in an increase from <1% to a 5% yield suggesting that DMF was not the source of the carboxylate of 8. Bubbling CO₂ gas through a standard reaction (entry 3) resulted in a 6% yield of 8, however, the most significant outcome from this reaction is the notably reduced yields of 4, 5, 6, and 7, and a

Scheme 5. Proposed Mechanism for Formation of 7 and 8

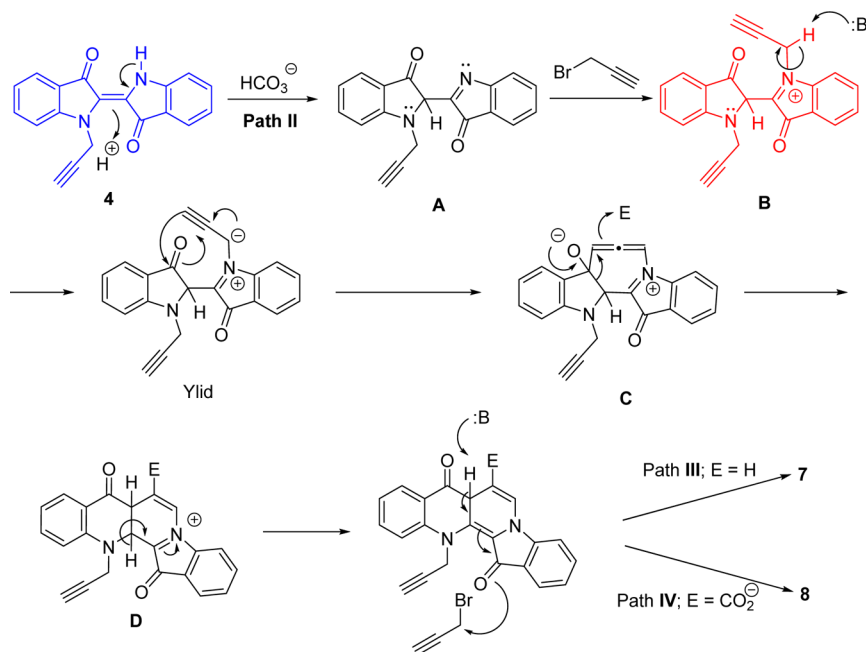
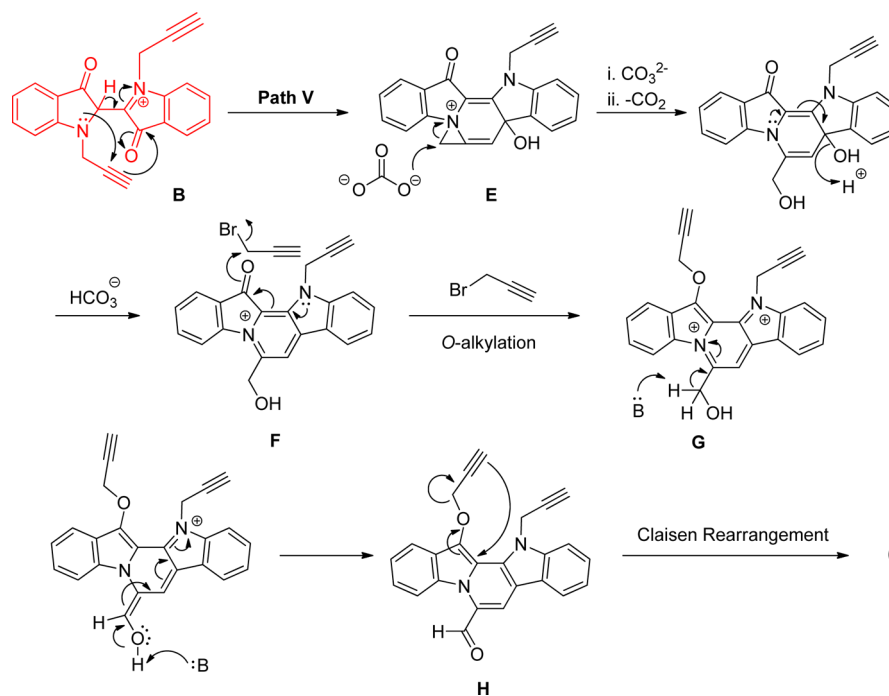


Table 1. Experiments to Probe the Source of the Ester Moiety 8

entry	solvent	other reaction conditions	4 yield %	5 yield %	6 yield %	7 yield %	8 yield %	baseline material (%mass)	recovered indigo (%mass)
1	DMF	Cs ₂ CO ₃ , N ₂	11	21	17	31	1	11	
2	DMSO	Cs ₂ CO ₃ , N ₂			12	13	5	65	
3	DMF	Cs ₂ CO ₃ , CO ₂	13		7	10	6	61	
4	DMF	K ₃ PO ₄ , N ₂	21						60
5	DMF	Cs ₂ CO ₃ , Ar	10	15	14	28	1	^a	

^aNot isolated.

Scheme 6. Proposed Mechanism for Formation of 6



dramatic increase in the production of noncharacterizable baseline material. This suggests that the presence of significant quantities of electrophiles could be reacting with different indigo-based nucleophiles as they are being generated resulting in mixtures of products. Entry 4 describes the experiment replacing the Cs₂CO₃ with K₃PO₄ as base, to eliminate the presence of a bicarbonate source. However, the lack of solubility of this base in DMF is the likely reason for the outcome of mostly unreacted indigo being isolated from the reaction.

Path V (Scheme 6) describes a possible mechanism to the allene **6** and diverges from the same intermediate **B** (red, Scheme 5). In this instance it is the iminium indigo moiety that activates the adjacent carbonyl, allowing sufficient electrophilicity to attract the relatively weak nucleophilic alkyne to undergo a cyclization reaction, promoted by the initial attack of the other indigo nitrogen lone electron pair onto the propargyl C2 in a concerted process yielding the strained fused-aziridine **E**. Carbonate could then act as a nucleophile in a ring-opening of the aziridine and subsequent aromatization of the central pyridinyl ring to give **F**. *O*-Propargylation of **F** could then afford intermediate **G**. The acidic proton in the CH₂OH group α to the iminium ion in **G** may then be removed under the influence of base and further OH proton loss would yield the aldehyde moiety in the intermediate **H**. A Claisen rearrangement of the propargyloxy group with the indolic C2–C3 bond could then give rise to product **6**.

The outcomes from this propargylation reaction are repeatable and preliminary investigations also indicate reliable scalability up to at least double quantities. Further, our mechanistic proposals for the formation of **6–8** all start from *N,N*-dipropargylated intermediates, rather than an intermediate that had cyclized initially from a *N*-monopropargylated molecule. In support of this proposal were the outcomes from an experiment where a DMF solution of **4** was dripped into a mixture of Cs₂CO₃ and propargyl bromide in DMF over 3 min before quenching after 2 min. The result was formation of **5** (<3%), **6** (11%), **7** (25%), and **8** (<1%) with complete consumption of the starting material. The poor return of **5** with respect to **6–8** suggests that the second *N*-propargylation is a more competitive reaction than cyclization, and lends support to our proposed dipropargylated compounds as intermediates.

It is also relevant to compare the mechanistic outcomes of this propargylation reaction with the outcomes of the corresponding allylation reaction (Scheme 1).⁹ Although cyclization onto the indigo carbonyl of the unsaturated moiety occurred in both instances, reaction onto the indigo C2 position to form a spiro compound only occurs in the case of the alkene. There was no evidence suggesting an equivalent mechanism pathway in the presence of the alkyne. Presumably, the linear alkyne is not able to approach the indigo C2 position whereas the “bent” nature of the alkene makes this cyclization reasonable. Further, a significant byproduct of the allylation reaction (Scheme 1) was *N*-allylisatin (structure not

illustrated), derived by oxidative cleavage of the central indigo double bond. Under propargylation conditions, there was no *N*-propargylisatin present, as evidenced by TLC analysis of the reaction mixture against an authentic sample.

We have also undertaken some simple experiments to ascertain that the reactions are likely to proceed through nucleophilic mechanisms rather than through radical-based sequences. Previous studies have shown that radical reactions with indigo will proceed exceptionally slowly at room temperature and in 4 h at 100 °C in the presence of oxygen and with irradiation.¹⁶ In contrast, we have repeated our propargylation reaction (as shown in Scheme 2) in the absence of oxygen and light (under argon) with these conditions realizing the same product outcome after 5 min of reaction at 86 °C. Radical reactions are unlikely to proceed under these conditions, let alone to produce a total yield of 84% of products in 5 min of reaction time.

The heterocycles **7** and **8** are analogs of the marine natural products faspaplysin and homofaspaplysin (Figure 2), initially

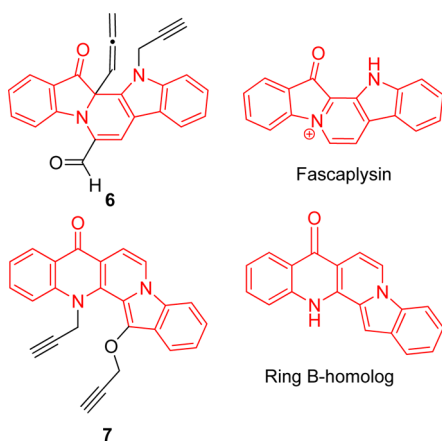


Figure 2. Representation of compounds **6** and **7** as analogs of faspaplysin/homofaspaplysin and faspaplysin/homofaspaplysin ring B-homologue, respectively.

isolated from the sponge *Faspaplysinopsis reticulata* with faspaplysin noted as an ATP-competitive inhibitor of Cdk4/D1 ($IC_{50} = 0.35 \mu M$)^{3,17} activity. There have been reported syntheses of these natural products including the silver-catalyzed cascade synthesis of their parent compound and analogs, with this approach involving the initial intermolecular reaction of two components of similar molecular complexity, however, this necessitated the prior synthesis of these two components.¹⁸ The B-ring homologue of faspaplysin has also been synthesized starting from 4(1*H*-indol-1-yl)butanoic acid in a 2 step synthesis in a best yield of 42%.¹⁹

We report here a facile synthesis of the benzoindolo[1,2-*h*][1,7]naphthyridine (faspaplysin) heterocyclic skeleton from indigo in the presence of propargyl bromide and base in a 17% unoptimized yield. This provides direct access to this skeleton starting from exceptionally cheap starting materials and reagents, and provides a convenient access to this system for further elaboration in structure–activity studies.

The reaction of indigo with propargyl bromide in the presence of base produces new complex heterocycles via a multistep, one-pot, cascade-type series of reactions. This is new science for the indigo moiety and represents an exciting untapped area of heterocyclic chemistry. Our proposed mechanisms (Schemes 4–6) reveal that at different stages of

the cascade reaction, the reactivity of different sites on the indigo moiety changes, and additionally, different types of reactivity can occur at different times, including sites acting as nucleophiles or electrophiles, with bond breakage leading to ring expansion and dehydration (Figure 3). A key element to

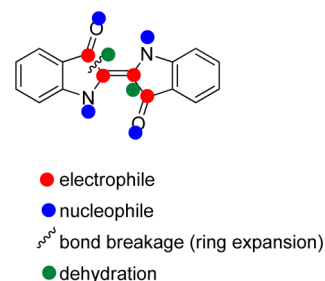


Figure 3. Graphical representation of the changing reactivity of the indigo skeleton with sites of nucleophilicity, electrophilicity, dehydration, and bond breakage illustrated. The degree of reactivity at each of these points changes as the molecule(s) progress through the cascade reaction.

the reactivity is the ability of the indigo heterocycle to tautomerize under different circumstances (e.g., upon generation of the *N*-centered anion with base) to shift reactivity to a different site. This constantly changing reactivity leads to the variety of outcomes as demonstrated. Further, this range of different chemistry all occurs in a tight cluster in the center of the indigo structure and this combination of properties is the key to the variety of unusual heterocycles that arises. Further, the unexpected outcomes of this initial study not only shows us that there is highly unusual and significant chemistry of indigo, but that there is much yet to be explored in this area.

Biological Testing. As an initial screen for biological activity, compounds **4**–**7** were subjected to *in vitro* antiplasmodial and anticancer testing (Table 2). All four compounds revealed notable antiplasmodial²⁰ activity against a drug-resistant strain in the micromolar range, sufficient for all to be considered lead compounds for further development.

More significantly, **4** (antiplasmodial IC_{50} 0.33 $\mu g/mL$, 1.1 μM) and **5** (antiplasmodial IC_{50} 0.256 $\mu g/mL$, 0.85 μM) are an order of magnitude more potent than compounds **6** and **7**. In the case of **4**, there was also a significant difference between the level of mammalian (Vero) cell toxicity (IC_{50} 16.26 $\mu g/mL$) and antiplasmodial activity (Table 1). With respect to the activity against cancer cells,²⁰ compounds **4**–**7** showed notable activity against the NCI-H187 lung cancer and KB-oral cavity cell lines. In particular, **7** was equipotent with the positive control ellipticine. Cytotoxicity²⁰ studies were particularly interesting for **5** and **6**, with the latter being noncytotoxic to normal mammalian cells but the former being toxic to these cells. Clearly, significant medicinal chemistry studies would need to be undertaken to decrease the toxicity to normal mammalian cells and increase the required selectivity. However, as a random screening process, all these compounds showed activity confirming that they could be considered as new lead compounds for a variety of targets.

CONCLUSION

We have reported here new cascade reactions of indigo via base-mediated propargylation. The resulting shifting of reactivity during each step in the process generates, and then propagates, a cascade reaction, producing a range of poly-

Table 2. Anti-Plasmodial and Anti-Cancer Activity of the Indigo-Derived Heterocycles 4–7

entry	compound	<i>Plasmodium falciparum</i> ^a antiplasmodial IC ₅₀ μg/mL (μM)	NCI-H187 lung anticancer IC ₅₀ μg/mL (μM)	KB-oral cavity anticancer IC ₅₀ μg/mL (μM)	cytotoxicity vero cell IC ₅₀ μg/mL (μM)
1	4	0.33 (1.1)	4.79 (15.9)	8.95 (29.8)	16.26 (54.2)
2	5	0.26 (0.85)	1.88 (6.24)	1.31 (4.36)	1.93 (6.43)
3	6	3.34 (8.9)	4.79 (12.7)	7.81 (20.7)	<i>b</i>
4	7	3.75 (9.9)	17.3 (46.0)	8.44 (22.34)	16.4 (43.6)
5	dihydroartemisinin/ mefloquine	0.24/0.03			
6	ellipticine/doxorubicin		1.21/0.108	1.04/0.674	

^aDrug resistant K1 strain. ^bNoncytotoxic.

heterocyclic compounds in unprecedented outcomes. Some of these compounds also hold promise as leads for the development of new antimalarial and anticancer agents. The scope for this reaction currently remains untapped, however, these initial studies suggest that the chemistry of indigo has significant potential for further development toward novel polycyclic compounds. The exploration of a variety of reaction types, inclusive of cascade processes, using indigo as a starting material remains an additional exciting area of synthetic chemistry to investigate. Interestingly, the possibility of using indirubin and isoindigo, as indigo analogs, in comparable cascade reactions remains unexplored and these starting materials also offer possibilities for the generation of new heterocycles in a one-pot process. These studies are currently underway in our laboratories.

EXPERIMENTAL SECTION

General Experimental Information. Reagents and solvents were purchased reagent grade and used without further purification unless otherwise stated. All reactions were performed in standard oven-dried glassware under a nitrogen atmosphere unless otherwise stated. Melting point temperatures are expressed in degrees Celsius (°C) and are uncorrected. ¹H and ¹³C NMR spectra (CHCl₃ solutions) were recorded at 500 and 125 MHz with chemical shifts (δ) reported in parts per million relative to TMS (δ = 0 ppm) or CDCl₃ (δ = 77.0 ppm) as internal standards. Coupling constants (*J*) are reported in Hertz (Hz). Multiplicities are reported as singlet (s), broad singlet (bs), doublet of doublets (dd), or multiplet (m). Electron impact (EI) mass spectra (MS) and electrospray (ESI single quadrupole) mass spectra have their ion mass to charge (*m/z*) values stated with their relative abundances as a percentage in parentheses. Peaks assigned to the molecular ion are denoted by M⁺ or M + 1. Infrared (IR) spectra were recorded on neat samples. UV-visible spectra were recorded with solutions of samples in CH₂Cl₂. Images from crystals were captured using stereo microscopes. All the images were provided from X-ray quality single crystals. Optical rotations were measured in CH₂Cl₂ solution at 25 °C. Thin layer chromatography (TLC) was performed using silica gel F254 aluminum sheets. Column chromatography was performed under gravity using silica gel 60 (0.063–0.200 mm). Eluents are in volume to volume (v:v) proportions. Solvent extracts or chromatographic fractions were concentrated by rotary evaporation in vacuo. Indigo (dye content 95%) was used without further purification. Petroleum spirit had a bp range of 40–60 °C.

Products from the Propargylation of Indigo. A suspension of powdered indigo (262 mg, 1.0 mmol) in anhydrous DMF (40 mL) was sonicated for 30 min and stirred vigorously under N₂ overnight. The resulting suspension was added to predried anhydrous cesium carbonate (1.20 g, 3.4 mmol) and molecular sieves (4 Å) while being stirred and warmed to 80–85 °C under a N₂ atmosphere. After 30 min propargyl bromide (0.595 mg, 5.0 mmol) was added and the reaction mixture was heated at 82–85 °C for 5 min. The mixture was filtered hot and then the solution was concentrated by rotary evaporation and the residue applied to a short plug of silica gel/celite (1:1) and washed

consecutively with 4 different solvent mixtures: 1, 70:30 CH₂Cl₂/petroleum spirit (250 mL); 2, CH₂Cl₂; 3, 50:50 CH₂Cl₂/EtOAc; and 4, 95:5 EtOAc/MeOH (250 mL). Four fractions were collected from the four different elutions. Fraction 1 was concentrated and slowly recrystallized in 9:1 petroleum spirit/EtOAc then filtered to yield 1-(prop-2-yn-1-yl)-[2,2'-biindolinylidene]-3,3'-dione 4 (33.00 mg, 11%) as a blue, papery solid. *R*_f (7:3 CH₂Cl₂/petroleum spirit) = 0.53, mp 267–269 °C; λ_{max}/nm (ε, M⁻¹cm⁻¹) 291 (10447), 634 (6381). IR (neat) ν_{max} 3278 (m), 1605 (s), 1463 (s), 1297 (s), 1066 (s), 1027 (s), 927 (m), 743 (m) cm⁻¹. ¹H NMR δ 2.17 (1H, s, H3''), 5.41 (1H, s, H1''), 6.96 (1H, t, *J* = 7.1 Hz, H5'), 6.99 (1H, d, *J* = 8.1 Hz, H7'), 7.09 (1H, t, *J* = 7.1 Hz, H5), 7.22 (1H, d, *J* = 8.1 Hz, H7), 7.48 (1H, t, *J* = 7.5 Hz, H6), 7.60 (1H, t, *J* = 7.5 Hz, H6'), 7.69 (1H, d, *J* = 7.5 Hz, H4'), 7.77 (1H, d, *J* = 7.5 Hz, H4) 10.60 (1H, s, H1). ¹³C NMR (CDCl₃) δ 37.1 (C1''), 72.5 (C3''), 78.4 (C2''), 111.5 (C7''), 111.9 (C7), 120.4 (C3'a), 120.9 (C5'), 121.5 (C5), 122.0 (C2'), 122.4 (C2), 125.0 (C4'), 125.1 (C4), 126.2 (C3a), 135.9 (C6), 136.4 (C6), 151.8 (C7'a), 152.6 (C7a), 187.6 (C3), 189.6 (C3'). MS (EI) *m/z*: 300 (100%, M⁺), 271 (53), 262 (32). HRMS (ESI) [M + H]⁺ calcd for C₁₉H₁₃N₂O₂, 301.0977; found, 301.0964.

The mother liquors from fraction 1 were combined with fraction 2 and then subjected to a silica gel column and elution with 7:3 CH₂Cl₂/petroleum spirit gave 13-oxo-12-(prop-2-yn-1-yl)-12b (propa-1,2-dien-1-yl)-12b,13-dihydro-12H-pyrido[1,2-*a*:3,4-*b'*]diindole-6-carbaldehyde 6 as yellow–orange crystals (63.92 mg, 17%). X-ray quality crystals were grown through slow crystallization from petroleum spirit/EtOAc (5:3). *R*_f (CH₂Cl₂) = 0.26, mp 229–231 °C; UV-vis (CH₂Cl₂) λ_{max}/nm (ε, M⁻¹cm⁻¹) 386 (12825), 244 (34151). IR (neat) ν_{max} 3278 (m), 1604 (s), 1463 (s), 1297 (m), 1065 (s), 1027 (s), 1015 (s), 743 (s) cm⁻¹. ¹H NMR δ 2.33 (1H, s, H3'), 4.79 (2H, d, *J* = 6.5 Hz, H3''), 5.42 (1H, t, *J* = 6.5 Hz, H1''), 5.51–5.66 (2H, m, H1'), 6.82 (1H, d, *J* = 8.4 Hz, H11), 6.94 (1H, t, *J* = 7.2 Hz, H3), 7.27 (1H, t, *J* = 7.6 Hz, H2), 7.35 (1H, t, *J* = 8.0 Hz, H9), 7.49 (1H, t, *J* = 8.0 Hz, H8), 7.54 (1H, d, *J* = 8.4 Hz, H10), 7.64–7.68 (2H, m, H1, H4), 7.65 (1H, s, H7), 9.62 (1H, s, 1''). ¹³C NMR (CDCl₃) δ 36.2 (C1'), 71.3 (C12b), 73.6 (C3'), 77.8 (C2'), 80.4 (C3''), 90.4 (C1''), 110.7 (C7a), 111.1 (C13a), 111.5 (C9), 113.6 (C1), 117.2 (C12a), 118.6 (C11), 121.1 (C3), 122.6 (C8), 124.1 (C10), 124.5 (C11a), 124.9 (C4), 131.8 (C7), 137.7 (C7b), 138.2 (C4a), 138.5 (C2), 158.6 (C6), 185.3 (C1''), 195.7 (C13), 208.4 (C2''). MS (EI) *m/z* 376 (5, M⁺), 371 (100%), 298 (24). HRMS (ESI) [M + H]⁺ calcd for C₂₅H₁₇N₂O₂, 377.1298; found, 377.1285.

Fraction 3 was recrystallized from CH₂Cl₂/petroleum spirit (1:9) giving 13-(prop-2-yn-1-yl)-14-(prop-2-yn-1-yloxy)benzo[*b*]indolo[1,2-*h*][1,7]naphthyridin-8-(13H)-one 7 (116.6 mg, 31%) as orange crystals. X-ray quality crystals were grown through slow crystallization from petroleum spirit/ethyl acetate (4:3). *R*_f (9:1 CH₂Cl₂/EtOAc) = 0.52, mp 218–220 °C; UV-vis (CH₂Cl₂) λ_{max}/nm (ε, M⁻¹cm⁻¹) 324 (27663), 441 (10360). IR (neat) ν_{max} 3205 (w), 1588 (m), 1485 (m), 1349 (m), 1260 (m), 1059 (m), 725 (s) cm⁻¹. ¹H NMR δ 2.14 (1H, t, *J* = 2.4 Hz, H3'), 2.30 (1H, t, *J* = 2.4 Hz, H3''), 4.74 (2H, d, *J* = 2.4 Hz, H1'), 5.49 (2H, d, *J* = 2.4 Hz, H1''), 7.33 (1H, d, *J* = 7.4 Hz, H7), 7.45 (3H, m, H1, H2, H3), 7.74–7.77 (1H, t, *J* = 7.8 Hz, H11), 7.85–7.90 (3H, m, H4, H10, H12), 8.01 (1H, d, *J* = 7.4 Hz, H6), 8.71 (1H, dd, *J* = 8.1, 1.4 Hz, H9). ¹³C NMR (CDCl₃) δ 44.0 (C1''), 63.7 (C1'), 74.5 (C3'), 76.5 (C3''), 78.5 (C2''), 78.6 (C2'), 104.0 (C7), 110.9

(C3), 117.9 (C7a), 118.6 (C12), 118.9 (C13b), 119.1 (C10), 119.9 (C6), 121.6 (C4a), 123.3 (C2), 123.9 (C2, C1, C4), 126.4 (C8a), 126.9 (C9), 129.3 (C14a), 132.6 (C11), 133.2 (C14), 139.1 (C13a), 143.5 (C12a), 175.8 (C8). MS (EI), m/z 376 (6, M⁺), 337 (100%), 309 (20), 298 (75). HRMS (ESI) [M + H]⁺ calcd for C₂₅H₁₇N₂O₂, 377.1285; found, 377.1302.

The mother liquor from the recrystallization of 7 was concentrated and then subjected to silica gel column chromatography, and elution with CH₂Cl₂/EtOAc (92:8) resulted in **prop-2-yn-1-yl 8-oxo-13-(prop-2-yn-1-yl)-14-(prop-2-yn-1-yloxy)-8,13-dihydrobenzo[b]-indolo[1,2-*h*][1,7]naphthyridine-7-carboxylate 8** (2 mg, <1%) as bright orange crystals. X-ray quality crystals were grown through slow crystallization from chloroform. R_f (9:1, CH₂Cl₂/EtOAc) = 0.59, mp 258–260 °C; IR (neat) ν_{\max} 3278 (m), 2925 (m), 1718 (s), 1595 (s), 1482 (m), 1237 (m), 1062 (m), 964 (m), 749 (s), 643 (s) cm⁻¹. ¹H NMR δ 2.14 (1H, bs, H3''), 2.30 (1H, bs, H3'''), 2.53 (1H, bs, H3'), 4.76 (2H, d, J = 2.0 Hz, H1''), 5.06 (2H, d, J = 1.7 Hz, H1'''), 5.43 (2H, d, J = 1.7 Hz, H1'), 7.43–7.50 (3H, m, H1, H2, H3), 7.75 (1H, t, J = 7.8 Hz, H11), 7.82–7.90 (3H, m, H4, H10, H12), 8.01 (1H, s, H6), 8.48–8.50 (1H, d, J = 7.8, H9). ¹³C NMR (CDCl₃) δ 44.1 (C1'''), 53.4 (C1'), 63.5 (C1''), 74.7 (C3'''), 75.1 (C3'), 76.5 (C3''), 77.9 (C2''), 78.1 (C2'), 78.2 (C2'''), 110.7 (C7a), 110.8 (C7), 112.2 (C3), 115.1 (C13b), 118.1 (C12), 118.7 (C10), 118.8 (C6), 122.0 (C4a), 123.8 (C2), 124.1 (C1), 124.7 (C4), 126.7 (C8a), 126.8 (C9), 130.0 (C14a), 133.6 (C11), 134.5 (C14), 139.2 (C13a), 142.9 (C12a), 167.1 (ester C=O) 174.5 (C8). MS (EI), m/z 458 (5, M⁺), 419 (100%), 380 (10), 375 (5), 337 (20), 298 (45). HRMS (ESI) [M + H]⁺ calcd for C₂₉H₁₉N₂O₄, 459.1345; found, 459.1363.

Fraction 4 was purified by preparative TLC using CH₂Cl₂/EtOAc (88:12) as the developing solvent and gave **6-methylene-6,7-dihydropyrazino[1,2-*a*:4,3-*a'*]diindole-13,14-dione 5** was isolated as a dark burgundy powder (63 mg, 21%. R_f (8.5:1.5, CH₂Cl₂/EtOAc) = 0.51, mp 280–284 °C. UV–vis (CH₂Cl₂) λ_{\max} /nm (ϵ , M⁻¹cm⁻¹) 324 (13088), 573 (6430). IR (neat) ν_{\max} 1701 (m), 1604 (m), 1470 (m), 1298 (m), 1185 (m), 1122 (s), 742 (s) cm⁻¹. ¹H NMR δ 4.41 (2H, s, H7), 5.04 (1H, H1'a), 5.38 (1H, H1'b), 6.95–7.00 (2H, m, H9, H11), 7.09 (1H, t, J = 7.4 Hz, H2), 7.48–7.55 (3H, m, H3, H4, H10), 7.73 (1H, d, J = 7.5 Hz, H12), 7.82 (1H, d, J = 7.5 Hz, H1). ¹³C NMR (CDCl₃) δ 45.9 (C7), 97.9 (C1'), 109.5 (C12), 112.7 (C4), 121.4 (C13a), 121.8 (C11), 122.7 (C2), 123.0 (C12a), 124.6 (C14a), 125.3 (C1), 125.5 (C6), 131.6 (C13b), 135.1 (C10), 135.5 (C3), 147.0 (C4a), 150.0 (C8a), 179.7 (C14), 180.8 (C13). MS (EI), m/z 300 (14), 207 (100%). HRMS (ESI) [M + H]⁺ calcd for C₁₉H₁₃N₂O₂, 301.0972; found, 301.0960.

1-(Prop-2-yn-1-yl)-[2,2'-biindolylidene]-3,3'-dione (4). A suspension of powdered indigo (262 mg, 1.0 mmol) in anhydrous DMF (50 mL) was sonicated for 60 min and stirred vigorously under N₂ overnight. The resulting suspension was added to predried anhydrous cesium carbonate (2.4 g, 7.42 mmol) and the mixture was stirred and warmed to 80–85 °C under a N₂ atmosphere. After 30 min propargyl bromide (1.90 mg 10.0 mmol) was added and the reaction mixture was heated at 82–85 °C for 5 s. The mixture was then poured into ice water and the resulting precipitate was filtered and recrystallized from petroleum spirit/EtOAc (90:10) to furnish **1-(prop-2-yn-1-yl)-[2,2'-biindolylidene]-3,3'-dione 4** (279.00 mg 93%) as a blue fluffy solid.

6-Methylene-6,7-dihydropyrazino[1,2-*a*:4,3-*a'*]diindole-13,14-dione (5). A solution of **4** (100 mg, 0.33 mmol) in anhydrous DMF (20 mL) was stirred and warmed to 80–85 °C under a N₂ atmosphere for 20 min. The solution was then added to predried anhydrous cesium carbonate (107 mg, 0.33 mmol) and was stirred and warmed at 80–85 °C under a N₂ atmosphere for 10 min. The mixture was then poured into ice water and the resulting precipitate was separated and subjected to silica gel short column chromatography and eluted with CH₂Cl₂/EtOAc (85:15) to give **6-methylene-6,7-dihydropyrazino[1,2-*a*:4,3-*a'*]diindole-13,14-dione 5** as a dark burgundy powder (98 mg, 98%).

Preparation of N-Propargylisatin. To a solution of isatin (147 mg, 1.00 mmol) in dry DMF (40 mL) was added cesium carbonate (650 mg, 2.00 mmol). The resulting brown suspension was stirred at

80–85 °C for 30 min and then propargyl bromide (119 mg, 1.00 mmol) was added under a N₂ atmosphere. The resulting mixture was stirred at 80–85 °C for 30 min, poured into ice water, and the suspension was partitioned between CH₂Cl₂ (20 mL) and water (20 mL). The aqueous layer was washed with CH₂Cl₂ (4 × 5 mL), and the combined organic layers were washed with water (3 × 10 mL), dried (MgSO₄), and concentrated. The residue was recrystallized from chloroform/hexane (1:6) to give **N-propargylisatin** (133 mg, 91%) as an orange solid. ¹H NMR (CDCl₃) δ 2.32 (2H, d, J = 1.7 Hz, H3'), 4.54 (2H, d, J = 1.9, H1'), 7.16 (2H, m, H5, H7), 7.66 (2H, m, H4, H6). ¹³C NMR (CDCl₃) δ 29.8 (C3'), 73.7 (C2'), 76.0 (C1'), 111.4 (C7), 118.0 (C3a), 124.5 (C5), 125.8 (C4), 138.8 (C6), 149.9 (C7a), 157.5 (C2), 182.9 (C3). MS (EI) m/z 185 (85%, M⁺), 129 (100%) consistent with literature values.²¹

Antiplasmodial Assay. The compounds and extracts were tested in vitro against *Plasmodium falciparum*, K1CB1 (K1), which is a multidrug resistant (chloroquine and antifolate resistant) strain, received as a generous gift from Professor Sodsri Thaitong, Chulalongkorn University, Bangkok, Thailand. The parasites were maintained in human red-blood cells in RPMI 1640 medium supplemented with 25 mM HEPES, 0.2% sodium bicarbonate, and 8% human serum at 37 °C in a 3% carbon dioxide gas incubator (Trager and Jensen, 1976). Samples were made up in DMSO solution and the in vitro antimalarial activity testing was carried out using the microdilution radioisotope technique. The test sample (25 μ L, in the culture medium) was placed in triplicate in a 96-well plate where parasitized erythrocytes (200 μ L) with a cell suspension (1.5%) of parasitemia (0.5–1%) were then added to the wells. The ranges of the final concentrations of the samples were varied from 2 × 10⁻⁵ to 1 × 10⁻⁷ M with 0.1% of the organic solvent. The plates were then cultured under standard conditions for 24 h after which ³H-hypoxanthine (25 μ L, 0.5 mCi) was added. The culture was incubated for 18–20 h after which the DNA from the parasite was harvested from the culture onto glass fiber filters and a liquid scintillation counter used to determine the amount of ³H-hypoxanthine incorporation.²² The inhibitory concentration of the sample was determined from its dose–response curves or by calculation.

Cancer Growth Inhibition and Vero Cell Toxicity Assay. Cancer growth inhibition assay and the Vero cell assay were performed using the Resazurin microplate assay (REMA) method as described by O'Brien et al.²³ In brief, cells at a logarithmic growth phase were harvested and diluted to 2.2 × 10⁴ cells/mL for KB and 3.3 × 10⁴ cells/mL for NCI-H187, in fresh medium. Successively, 5 μ L of test sample diluted in 5% DMSO, and 45 μ L of cell suspension were added to 384-well plates, incubated at 37 °C in 5% CO₂ incubator. After the incubation period (3 days for KB, and 5 days for NCI-H187), 12.5 μ L of 62.5 μ g/mL resazurin solution was added to each and the plates were then incubated at 37 °C for 4 h. Fluorescence signal was measured using SpectraMax M5 multidetection microplate reader (Molecular Devices, USA) at the excitation and emission wavelengths of 530 and 590 nm. Percent inhibition of cell growth was calculated by the following equation: % Inhibition = [1 – (FU_T/FU_C)] × 100 where FU_T and FU_C are the mean fluorescent unit from treated and untreated conditions, respectively. Dose–response curves were plotted from 6 concentrations of 3-fold serially diluted test compounds. Sample concentrations that inhibited cell growth by 50% (IC₅₀) were derived using the SOFTMax Pro software (Molecular Devices, USA). Ellipticine and doxorubicin were used as a positive control, and 0.5% DMSO and water were used as a negative control.²³

■ ASSOCIATED CONTENT

📄 Supporting Information

Copies of ¹H and ¹³C NMR for compounds 4–8 and UV–vis spectra for compounds 4–7, ORTEP plots and CIF files for 6, 7, and 8, images of fluorescence emission for 7 and 8, and a computed model for 5. This material is available free of charge via the Internet at <http://pubs.acs.org>.

■ AUTHOR INFORMATION

Corresponding Author

*Tel: +61 2 4221 4692. Fax: +61 2 4221 4287. E-mail: keller@uow.edu.au

Notes

The authors declare no competing financial interests.

■ ACKNOWLEDGMENTS

Financial support from the University of Wollongong, through the Centre for Medicinal Chemistry and a UPA scholarship to A.S. is gratefully acknowledged. We also thank Dr. Solomon Beckman for his help in the preparation of microscopic images of the crystals, and the Australian National University and BIOTEC for their support.

■ REFERENCES

- (1) (a) Anderson, E. A. *Org. Biomol. Chem.* **2011**, *9*, 3997–4006. (b) Shao, Z.; Peng, F. Z. *Curr. Org. Chem.* **2011**, *15*, 4144–4160.
- (2) Dančík, V.; Seiler, K. P.; Young, D. W.; Schreiber, S. L.; Clemons, P. A. *J. Am. Chem. Soc.* **2010**, *132*, 9259–9261.
- (3) Liu, W.; Khedkar, V.; Baskar, B.; Schürmann, M.; Kumar, K. *Angew. Chem., Int. Ed.* **2011**, *50*, 6900–6905.
- (4) (a) Gribble, G. W.; Pelcman, B. *J. Org. Chem.* **1992**, *57*, 3636–3642. (b) Carter, D. S.; Vranken, D. L. V. *J. Org. Chem.* **1999**, *64*, 8537–8545. (c) Segraves, N. L.; Robinson, S. J.; Garcia, D.; Said, S. A.; Fu, X.; Schmitz, F. J.; Pietraszkiewicz, H.; Valeriote, F. A.; Crews, P. *J. Nat. Prod.* **2004**, *67*, 783–792. (d) Dubovitskii, S. V. *Tetrahedron Lett.* **1996**, *37*, 5207–5208.
- (5) Bergman, J.; Koch, E.; Pelcman, B. *Tetrahedron* **1995**, *51*, 5631–5642.
- (6) Sasaki, T.; Ohtani, I. I.; Tanaka, J.; Higa, T. *Tetrahedron Lett.* **1999**, *40*, 303–306.
- (7) Lawrie, A. M.; Noble, M. E. M.; Tunnah, P.; Brown, N. R.; Johnson, L. N.; Endicott, J. A. *Nat. Struct. Mol. Biol.* **1997**, *4*, 796–801.
- (8) Bush, J. A.; Long, B. H.; Catino, J. J.; Bradner, W. T.; Tomita, K. *J. Antibiot.* **1987**, *40*, 668–678.
- (9) Abdel-Hamid, M. K.; Bremner, J. B.; Coates, J.; Keller, P. A.; Miländer, C.; Torkamani, Y. S.; Skelton, B. W.; White, A. H.; Willis, A. C. *Tetrahedron Lett.* **2009**, *50*, 6947–6950.
- (10) See Supporting Information, Figure S5 for illustrations of conformation.
- (11) Johnson, R. P. *Chem. Rev.* **1989**, *89*, 1111–1124.
- (12) Krause, A. N.; Hashmi, S. K. *Modern Allene Chemistry*, 1st ed.; Wiley-VCH: Weinheim, 2004; Vol. 1.
- (13) Daoust, K. J.; Hernandez, S. M.; Konrad, K. M.; Mackie, I. D.; Winstanley, J.; Johnson, R. P. *J. Org. Chem.* **2006**, *71*, 5708–5714.
- (14) Moemming, C. M.; Kehr, G.; Wibbeling, B.; Froehlich, R.; Schirmer, B.; Grimme, S.; Erker, G. *Angew. Chem., Int. Ed.* **2010**, *49*, 2414–2417.
- (15) Muzart, J. *Tetrahedron* **2009**, *65*, 8313–8323.
- (16) (a) Smith, B. D.; Alonso, D.; Bien, J. T.; Zielinski, J.; Smith, S. L.; Haller, K. J. *J. Org. Chem.* **1993**, *58*, 6493–6496. (b) Smith, B. D.; Haller, K. J.; Shang, M. *J. Org. Chem.* **1993**, *58*, 6905–6908. (c) Smith, B. D.; Alonso, D.; Bien, J. T.; Metzler, E. C.; Shang, M.; Roosenburg, J. M. *J. Org. Chem.* **1994**, *59*, 8011–8014.
- (17) Yan, X.; Chen, H.; Lu, X.; Wang, F.; Xu, W.; Jin, H.; Zhu, P. *Eur. J. Pharm. Sci.* **2011**, *42*, 251–259.
- (18) Waldmann, H.; Eberhardt, L.; Wittstein, K.; Kumar, K. *Chem. Commun.* **2010**, *7*, 4622–4624.
- (19) Baranova, O. V.; Zhidkov, M. E.; Dubovitskii, S. V. *Tetrahedron Lett.* **2011**, *52*, 2397–2398.
- (20) (a) Changsen, C.; Franzblau, S. G.; Palittapongarnpim, P. *Antimicrob. Agents Chemother.* **2003**, *47*, 3682–3687. (b) Desjardins, R. E.; Canfield, C. J.; Haynes, J. D.; Chulay, J. D. *Antimicrob. Agents Chemother.* **1979**, *16*, 710–718. (c) O'Brien, J.; Wilson, I.; Orton, T.; Pognan, F. *Eur. J. Biochem.* **2000**, *267*, 5421–5426.

(21) Radul, O. M.; Zhungietu, G. I.; Rekhter, M. A.; Bukhanyuk, S. M. *Khim. Geterotsikl. Soedin.* **1983**, *3*, 353–355.

(22) (a) Changsen, C.; Franzblau, S. G.; Palittapongarnpim, P. *Antimicrob. Agents Chemother.* **2003**, *47*, 3682–3687. (b) Desjardins, R. E.; Canfield, C. J.; Haynes, J. D.; Chulay, J. D. *Antimicrob. Agents Chemother.* **1979**, *16*, 710–718.

(23) O'Brien, J.; Wilson, I.; Orton, T.; Pognan, F. *Eur. J. Biochem.* **2000**, *267*, 5421–5426.